

## **Microstructural Modeling and Second-Order Two-Scale Computation for Mechanical Properties of 3D 4-Directional Braided Composites**

**Zihao Yang<sup>1</sup>, Junzhi Cui<sup>2</sup>, Yufeng Nie<sup>1</sup>, Yatao Wu<sup>1</sup>, Bin Yang<sup>3</sup>, and Bo Wu<sup>4</sup>**

**Abstract:** This study is concerned with the microstructural modeling and mechanical properties computation of three-dimensional (3D) 4-directional braided composites. Microstructure of the braided composite determines its mechanical properties and a precise geometry modeling of the composite is essential to predict the material properties. On the basis of microscopic observation, a new parameterized microstructural unit cell model is established in this paper. And this model truly simulates the microstructure of the braided composites. Furthermore, the mathematical relationships among the structural parameters, including the braiding angle, fiber volume fraction and braiding batch, are derived. By using the unit cell model, the second-order two-scale (SOTS) method is applied to predict the mechanical properties of 3D 4-directional braided composites, including stiffness parameters and strength parameters. Besides, the effects of the braiding angle and fiber volume fraction on the elastic constants are investigated in detail. Numerical results show that the predictive stiffness and strength parameters are in good agreement with the available experimental data, which demonstrate that the established unit cell model is applicable and the second-order two-scale method is valid to predict the mechanical properties of 3D 4-directional braided composites.

**Keywords:** 3D 4-directional braided composites, microstructural modeling, mechanical properties, the SOTS method.

---

<sup>1</sup> Department of Applied Mathematics, Northwestern Polytechnical University, Xi'an, 710072, China. E-mail: yzh@mail.nwpu.edu.cn.

<sup>2</sup> LSEC, ICMSEC, Academy of Mathematics and Systems Science, CAS, Beijing, 100190, China.

<sup>3</sup> Departement Temps-Fre quence, University of Franche-Comte, 26 chemin de l'Epitaphe, Besancon Cedex, 25030, France.

<sup>4</sup> GIPSA lab, UMR CNRS 5216, Grenoble University, Grenoble, 38400, France.

## 1 Introduction

3D braided composites are being widely used in the fields of aerospace, automobiles and marine due to their outstanding performance over conventional laminated composites, such as better structural integrity, low delaminating tendency and high damage tolerance. In order to apply the braided composites efficiently, safely and reasonably, it is important to evaluate the properties of the composites. However, due to the complicated microstructures, which greatly depend on the manufacturing process, such as braiding angle, volume fraction and pitch length, it is difficult to represent the mechanical properties of 3D braided composites. Therefore, in recent years, it becomes a hot topic to evaluate the mechanical properties of 3D braided composites, including stiffness parameters and strength parameters.

Microstructure of the braided composite determines its mechanical properties, and a precise geometry modeling of the composite is essential to accurately predict the properties. Up to now, many models have been developed for 3D 4-directional braided composites. Most of geometric models were proposed by describing the braiding yarns using the successive straight lines, such as fabric geometry model [Ko and Pastore (1985)], fiber interlock model [Ma, Yang and Chou (1986)], fiber inclination model [Yang, Ma and Chou (1986)] and three unit-cells model [Wu and Hao (1993)]. Furthermore, many current models were obtained by modifying and improving the three unit-cells model [Zhang and Xu (2012); Chen, Tao and Choy (1999)]. However, the yarn paths should be curved in the realistic braided composites. The microstructure in above models is very simplified and thus less precise results are obtained. And then, the lemniscate model [Wan, Li, Liang and Zhang (2005)] and helix geometry model [Kalidindi and Franco (1997)] were proposed. They are also simplified and could not reflect the real structure of braided composites. With the development of computer technology, the CAD becomes a powerful tool to establish the complicated structure, and some works have been done to establish the micro-geometric structure models by considering the curved braiding yarn paths [Wang, Zhang and Cheng (2008); Kang, Kim and Jung (2008)]. The latest review of microstructural modeling of 3D braided composites can be found in [Fang and Liang (2011); Wang and Xing (2010)]. More accurate microstructural models needs to be established and their effect on mechanical properties of 3D 4-directional braided composites requires to be further studied.

For the 3D braided composites, based on above micro-geometric models, a few theoretical methods have been developed to predict elastic constants, such as elastic strain energy approach [Ma, Yang and Chou (1986)], stiffness averaging method [Nagai, Yokoyama, Maekawa, Hamada and Noguchi (1992)], classical lamination theory method [Yang, Ma and Chou (1986)], three unit-cells model method [Wu and Hao (1993)] and mixed volume averaging technique [Wang and Wang (1995)].

Moreover, some experimental results for mechanical properties have also been obtained [Kalidindi and Abusafieh (1996); Yang (2002)], including tension, compression and bending. Although theoretical analysis is easy to implement, it can just obtain the elastic constants, and is difficult to exhibit the microscopic stress distribution and other mechanical characteristics of 3D braided composites. In addition, due to the variety of constitutes and the complexity of microstructure of 3D braided composites, it will take a long time and cost too much to do experiments. Thus the numerical simulation becomes more and more important because it can overcome those limitations existing in the theoretical and experimental analysis. Recently, some works have been focused on predicting the mechanical properties of 3D braided composites by using the finite element (FE) method [Zhang and Xu (2012); Chen, Tao and Choy (1999); Sun, Di, Zhang, Pan and Wu (2003); Pankow, Waas and Yen (2012)]. However, due to the complicated microstructure and sharply varying material coefficients, in order to capture microscopic stress distributions, the mesh size must be very small while employing the traditional FE method. Thus it leads to tremendous amount of computer memory and CPU time. Therefore, it is needed to developed new effective methods for predicting the mechanical properties of 3D 4-directional braided composites.

On the basis of homogenization method [Cioranescu and Donato (1999)], various multi-scale methods have been proposed [Guedes and Kikuchi (1990); Hou and Wu (1997)]. They only considered the first-order asymptotic expansions. In recent years, the second-order two-scale (SOTS) analysis method is introduced [Cui, Shin and Wang (1999)] to predict the physical and mechanical properties of periodic composites [Yu and Cui (2007); Cui and Yu (2006); Yang, Cui, Nie and Ma (2012)]. By the second-order correctors, the microscopic fluctuation of physical and mechanical behaviors inside the materials can be captured more accurately. In this paper, a new parameterized microstructural unit cell model is established, and it truly simulates the microstructure of the 3D 4-directional braided composite. According to the mathematical relationships among the structural parameters, including the curved yarn and its braiding angle, fiber volume fraction and braiding bitch, the parameterized design for the unit cell model is implemented by employing the UG software. And then based on the established model and the proper strength criterions of constituent materials, the mechanical parameters, including the stiffness and strength parameters, are predicted by using the second-order two-scale method. Besides, the effects of the braiding angle and fiber volume fraction on the elastic constants are also investigated in this paper.

The remainder of this paper is outlined as follows. In Section 2, the parametric modeling process of the unit cell of 3D 4-directional braided composites is discussed in detail. Section 3 is devoted to the formulation of the elasticity problem of

the braided composite by using the SOTS method, and the FE meshes of the composite are also given. The algorithm procedure of the SOTS method is stated and some numerical results for the mechanical properties of 3D 4-directional braided composites are shown in Section 4. Finally, it is concluded that the established unit cell model is applicable and the SOTS method is valid to predict the mechanical properties of 3D 4-directional braided composites.

## 2 Microstructure analysis and unit cell modeling

Microstructure of the braided composite determines its mechanical properties and a precise geometry modeling is essential to accurately predict the mechanical properties of the materials. 3D braided composites can be regarded as an assemblage of unit cell that captures the major features of the underlying microstructure and composition. And the main objective of this section is to develop a new unit cell model of 3D 4-directional braided composites prepared by four-step  $1 \times 1$  braiding technique.

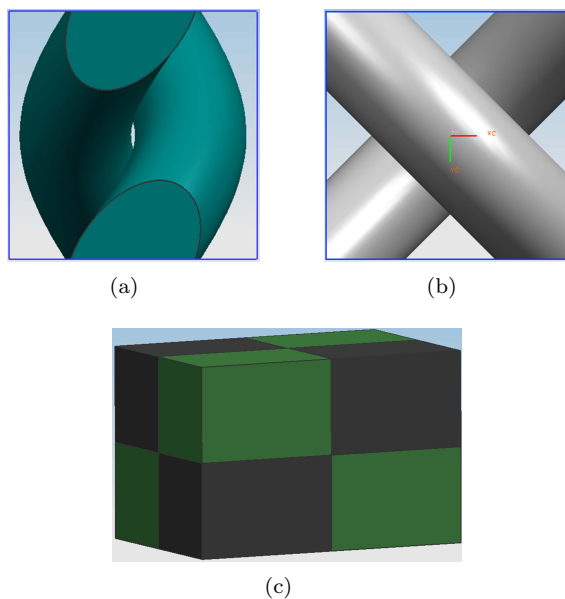


Figure 1: (a) Sub-cell A; (b) Sub-cell B; (c) Unit cell

The braided structure is supposed to be consistent. And the cross-section of the multifilament braiding yarns is circular. Moreover, suppose all yarns have identical constituent material. On the basis of the four-step  $1 \times 1$  braiding motion and micro-

scopic observation [Wang and Sun (2001)], the 3D 4-directional braided composites can be considered to be made of an infinite of two kinds of repeated sub-cells, A and B, as shown in Figs. 1(a) and 1(b). And sub-cell A and sub-cell B show the spatial directions of the braiding yarns. The arrangement of sub-cell A and sub-cell B in a unit cell is shown in Fig. 1(c) and they arrange alternatively in space. In addition, the yarns braiding along the horizontal direction ( $z$  direction) and the vertical direction ( $x$  or  $y$  direction) alternately in unit cell is shown in Fig. 2. Thus 3D 4-directional braided composite considered herein is assumed to be composed of the repeated unit cells.

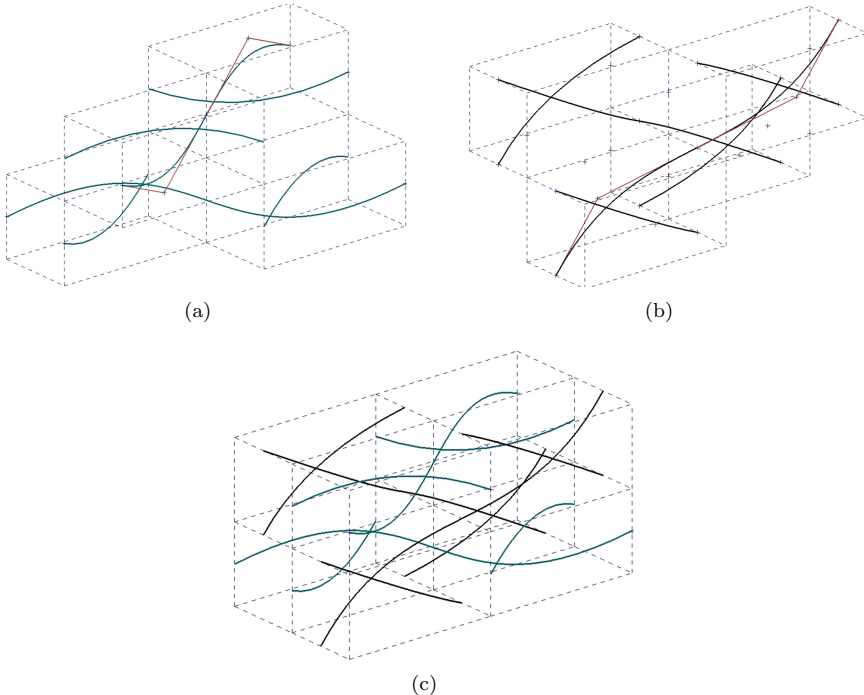


Figure 2: The yarns braiding along (a) the horizontal direction and vertical direction alternately; (b) the horizontal direction; (c) the vertical direction in unit cell

Fig. 3 shows the projection of yarn paths on the  $x$ - $z$  plane or  $y$ - $z$  plane. And the yarn orientation is characterized by the braiding angle  $\alpha$ , shown in Fig. 3. The length of the resultant unit cell is defined as the braiding pitch, denoted by  $l$ , and sub-cell A and B distribute alternatively every half of the pitch length along the direction of  $z$  axis.  $h$  stands for the width of the unit cell. According to the geometric relations as shown in Fig. 3, the following relations between the braiding angle, the width and

the pitch length of the unit cell are concluded

$$\tan \frac{\alpha}{2} = \frac{h}{l} \quad (1)$$

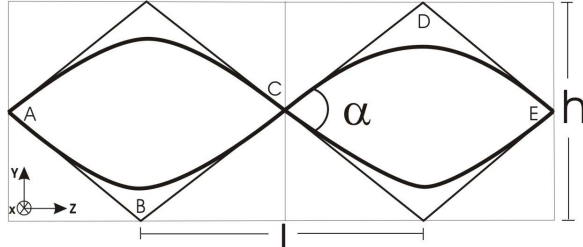


Figure 3: The cross-section of the 3D 4-directional braided composite

In this paper, the structural model of the unit cell is developed based on the UG software. And the spatial cubic spline function and the sweep function along the guideway provided by the UG software are utilized. During the modeling process, the width of the unit cell  $h$  is a constant. According to the relation (1), the braiding batch length  $l$  is obtained by specified braiding angle  $\alpha$ . Firstly, the path of braiding yarn is the yarn's centerline in 3D space and can be represented through a series of discrete control points coupling with the cubic spline interpolation function in UG. In this paper, the middle-points of the edges and the surfaces are chosen alternatively as the control points, as shown in Figs. 2 and 3. By using the interpolation function, the yarn's centerlines braiding along the horizontal direction and the vertical direction alternately in unit cell are obtained as shown in Fig. 2. Next, by setting the radius of the circular cross-section and utilizing the sweep function along the guideway, the solid structure model of fibers is established as shown in Fig. 4(a). Furthermore, a rectangular object is created in the whole domain of unit cell. And solid structural models of unit cell are realized by Boolean operations between the rectangular object and the fibers' solid structure object, as shown in Fig. 4(b). Besides, it is noteworthy that a unit cell intersects with the fibers of its adjacent unit cells. Therefore, to avoid omitting the information of the fibers when implementing Boolean operations, fibers of the adjacent unit cells should be created when establishing the fibers of the unit cell.

Fig. 2(a) shows that there are 12 yarns in unit cell, which are braiding along the horizontal direction and vertical direction, respectively. As is seen from Figs. 2(b) and 2(c), the yarns braiding along the horizontal direction and the vertical direction

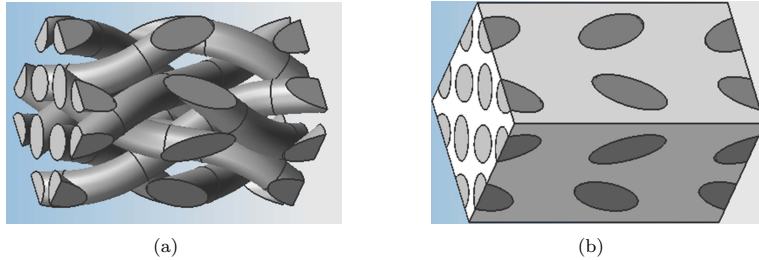


Figure 4: Solid Structure models of (a) fibers and (b) the entire unit cell

can be divided into two groups, respectively. Thus the 12 yarns are divided into four groups and the yarns belonging to the same group have similar yarn paths. Besides, there exists intersection between a unit cell and the fibers of its adjacent unit cells, and the intersection includes eight blocks of fibers, which are divided into four groups as shown in Fig. 4(a). So the whole fibers in a unit cell can be divided into four groups and the fibers in the same group are shown in Fig. 5(a). After translation, two complete fibers are obtained as shown in Fig. 5(b).  $r$  denotes the radius of the yarn and the fiber volume  $V_f$  is obtained as follows

$$V_f = \pi r^2 l_f \quad (2)$$

where  $l_f$  is the length of the fibers in unit cell. Moreover, the volume of unit cell  $V_c$  is calculated by

$$V_c = h^2 l \quad (3)$$

And the fiber volume fraction is

$$\nu = \frac{V_f}{V_c} = \frac{\pi r^2}{h^2} \frac{l_f}{l} \quad (4)$$

Based on previous microstructure analysis, we know from (4) that  $l_f/l$  is only related to the braiding angle, and it reflects the internal relations between the fiber volume fraction and the braiding angle.

From the mathematical relationship between the structural parameters, the input parameters to generate the unit cell models are identified as the braiding angle

and the fiber volume fraction. And other parameters can be determined by them. Parameterized unit cell models are beneficial to parameters modification and model regeneration. As a result, UG is exploited secondly by Microsoft Visual Studio and the parameterized modeling of the unit cell of 3D 4-directional braided composite with different braiding angle and different fiber volume fraction is realized.

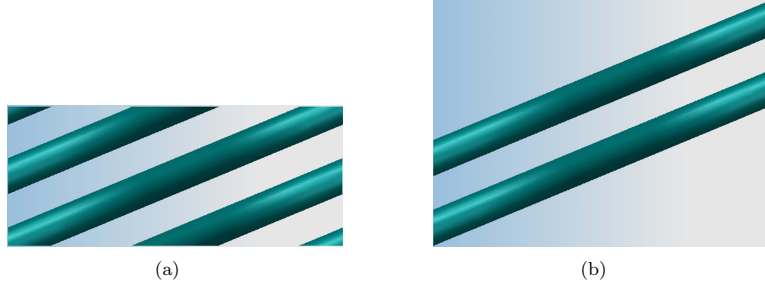


Figure 5: (a) A group of fibers; (b) the fibers after translation

### 3 Second-order two-scale method

#### 3.1 Second-order two-scale formulation

From solid mechanics, the elasticity problem of the structures made from 3D 4-directional braided composites can be expressed as follows

$$\begin{cases} \frac{\partial}{\partial x_j} \left( C_{ijk}^{\varepsilon}(x) \frac{1}{2} \left( \frac{\partial u_h^{\varepsilon}(x)}{\partial x_k} + \frac{\partial u_k^{\varepsilon}(x)}{\partial x_h} \right) \right) = f_i(x) & x \in \Omega \\ \mathbf{u}^{\varepsilon}(x) = \bar{\mathbf{u}}(x) & x \in \Gamma_1 \\ \sigma(u) \equiv v_j C_{ijk}^{\varepsilon}(x) \frac{1}{2} \left( \frac{\partial u_h^{\varepsilon}(x)}{\partial x_k} + \frac{\partial u_k^{\varepsilon}(x)}{\partial x_h} \right) = p_i(x) & x \in \Gamma_2 \\ \Gamma_1 \cap \Gamma_2 = \emptyset, \quad \Gamma_1 \cup \Gamma_2 = \partial \Omega \end{cases} \quad (5)$$

where  $i, j, k, l = 1, 2, 3$ ;  $\Omega$  is composed of entire  $\varepsilon$ -size cells, shown in Fig. 6;  $\mathbf{u}^{\varepsilon}(x)$  is the displacement solution vector;  $f_i(x)$  is a body force independent of  $\varepsilon$ ;  $C_{ijk}^{\varepsilon}(x)$  are the elastic coefficients;  $\Gamma_1$  and  $\Gamma_2$  denote boundaries of  $\Omega$  where displacement  $\bar{\mathbf{u}}(x)$  and loads  $p_i(x)$  are prescribed, respectively;  $v_j$  are the normal direction cosines of  $\Gamma_2$ .

Let  $y = x/\varepsilon \in Y$  denotes the local coordinates on the unit cell. Then  $\mathbf{u}^{\varepsilon}(x) = \mathbf{u}(x, y)$  and  $C_{ijk}^{\varepsilon}(x) = C_{ijk}(y)$ . From [Yu and Cui (2007); Cui and Yu (2006)], the second-order two-scale approximate solution can be expressed as

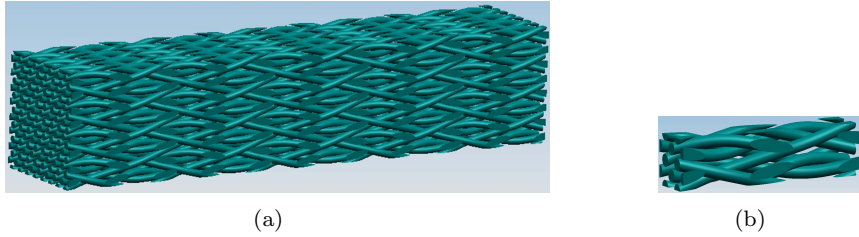


Figure 6: 3D braided composite structures (a) The macrostructure ; (b) unit cell

$$\mathbf{u}^\varepsilon(x) = \mathbf{u}_0(x) + \sum_{l=1}^2 \varepsilon^l \sum_{\alpha_1 \dots \alpha_l=1,2,3} \mathbf{N}_{\alpha_1 \dots \alpha_l}(y) \frac{\partial^l \mathbf{u}_0(x)}{\partial x_{\alpha_1} \dots \partial x_{\alpha_l}} \quad (6)$$

where  $\mathbf{u}_0(x)$  is the homogenized solution defined on  $\Omega$ ,  $\mathbf{N}_{\alpha_1}(y)$  and  $\mathbf{N}_{\alpha_1 \alpha_2}(y)$  are matrix-valued functions defined on the unit cell  $Y$ . And  $\mathbf{N}_{\alpha_1}(y)$ ,  $\mathbf{N}_{\alpha_1 \alpha_2}(y)$  and  $\mathbf{u}_0(x)$  are determined in the following ways

1) For  $l = 1$ ,  $\mathbf{N}_{\alpha_1 m}(y)$  ( $\alpha_1, m = 1, 2, 3$ ) are solutions of the following problem

$$\begin{cases} -\frac{\partial}{\partial y_j} \left[ C_{ijkh}(y) \frac{1}{2} \left( \frac{\partial \mathbf{N}_{\alpha_1 km}(y)}{\partial y_h} + \frac{\partial \mathbf{N}_{\alpha_1 hm}(y)}{\partial y_k} \right) \right] = \frac{\partial}{\partial y_j} (C_{ijm\alpha_1}(y)), y \in Y \\ \mathbf{N}_{\alpha_1 m}(y) = 0, y \in \partial Y \end{cases} \quad (7)$$

2) From  $\mathbf{N}_{\alpha_1 m}(y)$  ( $\alpha_1, m = 1, 2, 3$ ), the homogenized parameters  $\hat{C}_{ijhk}$  are calculated by the following formula

$$\hat{C}_{ijhk} = \frac{1}{|Y|} \int_Y \left( C_{ijhk}(y) + C_{ijm\alpha_1}(y) \frac{1}{2} \left( \frac{\partial \mathbf{N}_{hmk}(y)}{\partial y_{\alpha_1}} + \frac{\partial \mathbf{N}_{h\alpha_1 k}(y)}{\partial y_m} \right) \right) dy \quad (8)$$

3)  $\mathbf{u}_0(x)$  is the solution of the homogenized problem with above homogenized parameters defined as follows

$$\begin{cases} \frac{\partial}{\partial x_j} \left( \hat{C}_{ijhk} \frac{1}{2} \left( \frac{\partial u_{0h}(x)}{\partial x_k} + \frac{\partial u_{0k}(x)}{\partial x_h} \right) \right) = f_i(x) & x \in \Omega \\ \mathbf{u}_0(x) = \bar{\mathbf{u}}(x) & x \in \Gamma_1 \\ \boldsymbol{\sigma}(u) \equiv v_j \hat{C}_{ijhk} \frac{1}{2} \left( \frac{\partial u_{0h}(x)}{\partial x_k} + \frac{\partial u_{0k}(x)}{\partial x_h} \right) = p_i(x) & x \in \Gamma_2 \\ \Gamma_1 \cap \Gamma_2 = \emptyset, \quad \Gamma_1 \cup \Gamma_2 = \partial \Omega \end{cases} \quad (9)$$

4) For  $l = 2$ ,  $\mathbf{N}_{\alpha_1 \alpha_2 m}(y)$  ( $\alpha_1, \alpha_2, m = 1, 2, 3$ ) are solutions of the following problem

$$\begin{cases} -\frac{\partial}{\partial y_j} \left[ C_{ijhk}(y) \frac{1}{2} \left( \frac{\partial \mathbf{N}_{\alpha_1 \alpha_2 km}(y)}{\partial y_h} + \frac{\partial \mathbf{N}_{\alpha_1 \alpha_2 hm}(y)}{\partial y_k} \right) \right] = \\ \frac{\partial}{\partial y_j} (C_{ijk\alpha_2}(y) \mathbf{N}_{\alpha_1 km}(y)) + C_{i\alpha_1 kj}(y) \frac{\partial \mathbf{N}_{\alpha_2 km}(y)}{\partial y_j}, y \in Y \\ + C_{i\alpha_1 m\alpha_2}(y) - \hat{C}_{i\alpha_1 m\alpha_2} \\ \mathbf{N}_{\alpha_1 \alpha_2 m}(y) = 0, \quad y \in \partial Y \end{cases} \quad (10)$$

Further, the strains inside the structure  $\Omega$  can be calculated by the following formula

$$\begin{aligned} \boldsymbol{\varepsilon}_{hk}(x, y) &= \frac{1}{2} \left( \frac{\partial u_h^0(x)}{\partial x_k} + \frac{\partial u_k^0(x)}{\partial x_h} \right) \\ &+ \sum_{l=1}^2 \boldsymbol{\varepsilon}^{l-1} \sum_{<\alpha>=l} \frac{1}{2} \left[ \frac{\partial N_{\alpha hm}(y)}{\partial y_k} + \frac{\partial N_{\alpha km}(y)}{\partial y_h} \right] D_\alpha^l u_m^0(x) \\ &+ \sum_{l=1}^2 \boldsymbol{\varepsilon}^l \sum_{<\alpha>=l} \frac{1}{2} \left[ N_{\alpha hm}(y) D_{\alpha k}^{l+1} u_m^0(x) + N_{\alpha km}(y) D_{\alpha h}^{l+1} u_m^0(x) \right] \end{aligned} \quad (11)$$

And from Hooke's law, the stresses inside  $\Omega$  are calculated by

$$\sigma_{ij}(x, y) = C_{ijhk}(y) \boldsymbol{\varepsilon}_{hk}(x, y) \quad (12)$$

In this paper, we consider two kinds of typical components, the tensional or compressive column and the bending beam, to evaluate the mechanical properties of braided composite structures. Since the homogenization parameters of previous typical components made from braided composites have orthogonal-anisotropic properties, from solid mechanics, it is easy to get the exact solution of their displacement. Thus, the exact expressions of the displacements, strains and stresses for those components can be obtained.

1) Column tension/compression. For tension or compression behavior of the column with rectangle cross section in the axial direction, as shown in Fig. 7(a), the homogenization displacement can be expressed as

$$u_{01} = -\frac{v_{13}}{E_{11}} p x_1, \quad u_{02} = -\frac{v_{23}}{E_{22}} p x_2, \quad u_{03} = -\frac{p}{E_{33}} p x_3 \quad (13)$$

where  $p = T/A$ ;  $E_{11}$ ,  $E_{22}$ ,  $E_{33}$ ,  $v_{13}$  and  $v_{23}$  are the homogenized elasticity parameters of three axis directions. Thus, the displacement and strain can be expressed as

$$\mathbf{u}^\varepsilon(x) = \mathbf{u}_0(x) + \varepsilon \mathbf{N}_{\alpha_1}(y) \frac{\partial \mathbf{u}_0(x)}{\partial x_{\alpha_1}} \quad (14)$$

$$\begin{aligned} \boldsymbol{\varepsilon}_{hk}(x, \frac{x}{\varepsilon}) &= \frac{1}{2} \left( \frac{\partial u_h^\varepsilon(x)}{\partial x_k} + \frac{\partial u_k^\varepsilon(x)}{\partial x_h} \right) = \frac{1}{2} \left( \frac{\partial u_{0h}(x)}{\partial x_k} + \frac{\partial u_{0k}(x)}{\partial x_h} \right) \\ &+ \frac{1}{2} \left( \frac{\partial N_{\alpha_1 hm}(y)}{\partial y_k} + \frac{\partial N_{\alpha_1 km}(y)}{\partial y_h} \right) \frac{\partial u_{0m}(x)}{\partial x_{\alpha_1}} \end{aligned} \quad (15)$$

2) Beam bending. For the bending of a beam with rectangle cross section, shown in Fig. 7(b), the homogenization displacement can be expressed as

$$\begin{aligned} u_{01} &= -\frac{M}{2I_{x_2}} \left( \frac{1}{E_{33}} x_3^2 + \frac{v_{13}}{E_{11}} x_1^2 - \frac{v_{23}}{E_{22}} x_2^2 \right) \\ u_{02} &= -\frac{v_{23}M}{E_{22}I_{x_2}} x_1 x_2, \quad u_{03} = \frac{M}{E_{33}I_{x_2}} x_1 x_3 \end{aligned} \quad (16)$$

where  $I_{x_2} = bh^3/12$  is the moment of inertia round  $x_2$ . Thus, the displacement and strain are calculated by the following formulas

$$\mathbf{u}^\varepsilon(x) = \mathbf{u}_0(x) + \varepsilon \mathbf{N}_{\alpha_1}(y) \frac{\partial \mathbf{u}_0(x)}{\partial x_{\alpha_1}} + \varepsilon^2 \mathbf{N}_{\alpha_1 \alpha_2}(y) \frac{\partial^2 \mathbf{u}_0(x)}{\partial x_{\alpha_1} \partial x_{\alpha_2}} \quad (17)$$

$$\begin{aligned} \boldsymbol{\varepsilon}_{hk}(x, \frac{x}{\varepsilon}) &= \frac{1}{2} \left( \frac{\partial u_h^\varepsilon(x)}{\partial x_k} + \frac{\partial u_k^\varepsilon(x)}{\partial x_h} \right) = \frac{1}{2} \left( \frac{\partial u_{0h}(x)}{\partial x_k} + \frac{\partial u_{0k}(x)}{\partial x_h} \right) \\ &+ \frac{1}{2} \left( \frac{\partial N_{\alpha_1 hm}(y)}{\partial y_k} + \frac{\partial N_{\alpha_1 km}(y)}{\partial y_h} \right) \frac{\partial u_{0m}(x)}{\partial x_{\alpha_1}} \\ &+ \varepsilon \frac{1}{2} \left( N_{\alpha_1 hm}(y) \frac{\partial^2 u_{0m}(x)}{\partial x_{\alpha_1} \partial x_k} + N_{\alpha_1 km}(y) \frac{\partial^2 u_{0m}(x)}{\partial x_{\alpha_1} \partial x_h} \right) \\ &+ \varepsilon \frac{1}{2} \left( \frac{\partial N_{\alpha_1 \alpha_2 hm}(y)}{\partial y_k} + \frac{\partial N_{\alpha_1 \alpha_2 km}(y)}{\partial y_h} \right) \frac{\partial^2 u_{0m}(x)}{\partial x_{\alpha_1} \partial x_{\alpha_2}} \end{aligned} \quad (18)$$

Further, using the stress-strain relation, one can evaluate the stresses anywhere inside the column and beam.

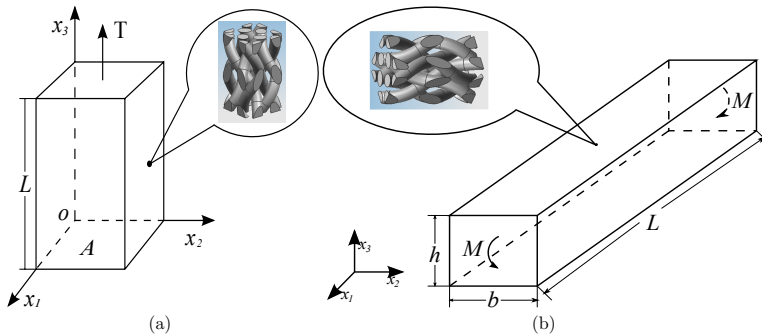


Figure 7: (a) Axial tension/compression of a column with rectangle cross section; (b) pure bending of a beam with rectangle cross section

### 3.2 Strength analysis of the 3D 4-directional braided composites

As the distributions of the strain and stress inside the investigated structure made from 3D 4-directional braided composite materials are obtained in previous section, proper strength criterions are expected for the elasticity strength analysis. But until now, there is no strength criterion specialized for the braided composites. Due to the wide difference in the mechanical properties between the fibers and matrix of the composite, different conventional strength criterions of homogenous materials should be employed for them, respectively. And the strength criterions adopted in this paper are described as follows.

1) As a brittle material, the fibers are always subjected to the longitudinal load and their fracture occurs along the transverse section. And the fibers can be considered as transversely isotropic linear elastic materials. Hence, in this paper, the longitudinal normal stress is taken and the criterion can be expressed as

$$\sigma_L < S_L, \quad (19)$$

where \$\sigma\_L\$ is the longitudinal normal stress and \$S\_L\$ is the longitudinal elasticity limit stress.

2) The matrix is always considered as an isotropic and ductile material and the generalized Von-Mises stress yield criterion adopted is expressed as follows

$$\sigma_e = \frac{1}{\sqrt{2}} \sqrt{(\sigma_{11} - \sigma_{22})^2 + (\sigma_{22} - \sigma_{33})^2 + (\sigma_{33} - \sigma_{11})^2 + 6(\sigma_{12}^2 + \sigma_{23}^2 + \sigma_{31}^2)} < S_e \quad (20)$$

where  $\sigma_{ij}$  ( $i, j = 1, 2, 3$ ) are the components of the stress tensor obtained from (12),  $\sigma_e$  the strength of the matrix,  $S_e$  the tensile or compressive elasticity limit stress.

Consequently, if and only if above inequalities do not hold, the corresponding constituent material is considered to be in a yielding state. And then the component made of the 3D 4-directional braided composite can be thought to reach the elasticity strength limit.

### 3.3 Finite element meshes

The efficiency and quality to generate meshes have important influence on the efficiency and precision of SOTS calculation. Due to the complexity of the geometry model of the 3D 4-directional braided composite developed in this paper, the ICEM software package was used to generate the FE meshes of the model. The geometry model of the unit cell developed by using the UG software was imported into ICEM software, and then the model with the fiber volume fraction 45% and braiding angle  $43^\circ$  was meshed by 6478 tetrahedron elements shown in Fig. 8.

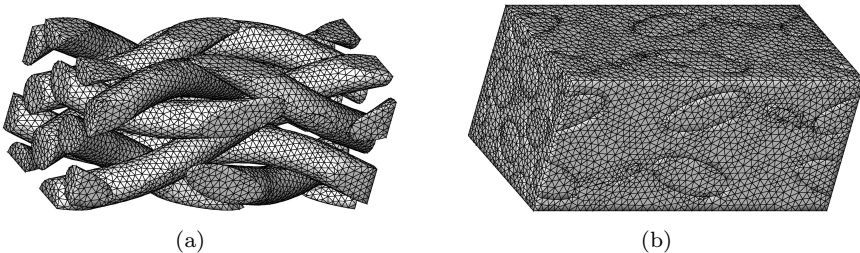


Figure 8: FE meshes of the unit cell of 3D 4-directional braided composite. The meshes of (a) fibers and (b) the entire unit cell

## 4 FE algorithm and numerical examples

In this section, the algorithm procedure of the SOTS method for predicting the mechanical properties of 3D 4-directional braided composite materials is presented, and some numerical examples are given.

### 4.1 Algorithm procedure of SOTS method based on FE computation

Based on the representation, geometry modeling and FE mesh generation of 3D 4-directional braided composite in previous sections, the algorithm procedure of the SOTS method for predicting the mechanical properties of the composites is stated as follows

1. Generate a geometry model of the unit cell according to the given fiber volume fraction  $v$  and braided angle  $\alpha$  by means of the microstructural modeling method in section 2, and determine the material coefficients of the fibers and matrix. And then generate its FE meshes.
2. Solve the problem (7) by using the FE method to obtain the FE solutions of  $\mathbf{N}_{\alpha_1 m}(y)$  ( $\alpha_1, m = 1, 2, 3$ ), and then calculate the homogenized coefficient  $\hat{C}_{ijk}$  by the formula (8).
3. With the homogenized coefficients obtained in step 2, the homogenization solution  $\mathbf{u}_0(x)$  can be obtained by solving problem (9). For some typical structures,  $\mathbf{u}_0(x)$  can be exactly obtained from the solid mechanics.
4. Solve the problem (10) by using the same FE meshes as in step 2 to obtain the FE solutions of  $\mathbf{N}_{\alpha_1 \alpha_2 m}(y)$ .
5. From the homogenization displacement  $\mathbf{u}_0(x)$ , the macroscopic distributions of the strain and stress inside the investigated component can be evaluated without considering the detailed configuration of unit cells. Thus we can determine the macroscopic dangerous area of the investigated component, i.e. the area where the stress or strain reaches the maximum. And then we can evaluate the strain and stress fields inside the unit cells within the macroscopic dangerous area by using formulas (11) and (12).
6. Determine the critical load for the previous two typical components by applying the strength criterions given in section 3.2 to the fibers and matrix of the unit cells within the macroscopic dangerous area anywhere. After that, based on the critical load and homogenization coefficients, the elasticity strength limit of the component made of the 3D 4-directional braided composite is determined.

## 4.2 Numerical examples

### 4.2.1 Comparison with experimental results

In this section, the predictive results evaluated by the SOTS method are compared with the experimental data [Lu, Feng, Kou, Liu, Lu, Mai and Tang (1999); Yan, Wu and Sun (2007); Wang, Jiao, Tao and Geng (2003)] for the mechanical properties of 3D 4-directional braided composites. The elastic properties of the constituent materials, including T300 carbon fiber, TDE-8 epoxy resin and QY9512 bismaleimide resin, are listed in Table 1. And Table 2 summaries the structural parameters of the samples.

Table 3 present the SOTS results of the axial tensile elastic modulus and tensile strength against the experimental data of [Lu, Feng, Kou, Liu, Lu, Mai and Tang (1999)]. Comparison of the axial compressive modulus and compressive strength predicted by the SOTS method and the measured results from [Yan, Wu and Sun (2007)] is shown in Table 4. And Table 5 gives the predicted results and the measured bending strength cited from [Wang, Jiao, Tao and Geng (2003)]. It can be seen from Tables 3-5 that there is a good agreement between the experimental data and SOTS results, including the axis tensile and compressive modulus, the tensile, compressive and bending strength, for all the five samples studied. And the results demonstrate that the present model is applicable and the SOTS method is valid to predict the mechanical properties of 3D 4-directional braided composites.

Table 1: Elastic properties of constituent materials

Material	$E_{f1}$ (GPa)	$E_{f2}$ (GPa)	$G_{f12}$ (GPa)	$\mu_{f23}$	$\mu_{f12}$	$E_m$ (GPa)	$\mu_m$
T300	220	13.8	9.0	0.25	0.2	—	—
TDE-8	—	—	—	—	—	4.5	0.34
QY9512	—	—	—	—	—	3.4	0.34

Table 2: Structural parameters of the samples

Sample number	Materials	Braiding angle( $^{\circ}$ )	Fiber volume fraction(%)
1	T300/TDE-8	21	45.0
2	T300/TDE-8	48	45.0
3	T300/TDE-8	16	38.9
4	T300/TDE-8	27	33.9
5	T300/QY9512	25	59.0

#### 4.2.2 Discussion on the effective elastic properties

After comparing the SOTS results obtained from using the present model with the experimental data, the effects of the braiding angle and the fiber volume fraction on the effective elastic constants are studied in this section. The mechanical properties for the carbon fiber constitute and epoxy resins are listed in Table 6. Figs. 9(a) and 9(b) show the variation of the effective elastic constants with the braiding angle

Table 3: Comparison of SOTS result and tensile experimental data [Lu, Feng, Kou, Liu, Lu, Mai and Tang (1999)]

Sample number	Axial elastic modulus (GPa)		Error (%)	Tensile strength (MPa)		Error (%)		
	Measured	Predicted		Measured	Predicted			
1	70.4	67.4	4.3	665.0	649.5	2.3		
2	25.0	23.5	6.0	254.0	260.1	2.4		

Table 4: Comparison of SOTS result and compressive experimental data [Yan, Wu and Sun (2007)]

Sample number	Axial elastic modulus (GPa)		Error (%)	Compressive strength (MPa)		Error (%)		
	Measured	Predicted		Measured	Predicted			
3	65.1	67.4	3.5	445.5	435.6	2.2		
4	36.1	33.6	6.9	198.9	201.6	1.4		

Table 5: Comparison of SOTS result and bending experimental data [Wang, Jiao, Tao and Geng (2003)]

Sample number	Bending strength (MPa)		Error (%)
	Measured	Predicted	
5	954	928	2.7

under the fiber volume fraction 45%. And Figs. 9(c) and 9(d) show the variation of the elastic constants with the fiber volume fraction under the braiding angle 15°. It is easy to see from Fig. 9(a) that there is a drop for the elastic modulus  $E_z$  as the increment of the braiding angle. And the reason for this is that the yarns load bearing in the longitudinal direction decreases as the braiding angle increases. Besides, Fig. 9(c) illustrates that the elastic modulus  $E_z$  increases with the increment of the fiber volume fraction. Figs. 9(b) and 9(d) present that the transverse Poisson's ratio  $V_{xy}$  varies with respect to the braiding parameters. It can be seen that  $V_{xy}$  firstly decreases and then increases with the increase of the braiding angle. And the minimum value of  $V_{xy}$  is obtained when the braiding angle is about 25°. Moreover,  $V_{xy}$  decreases as the fiber volume fraction increases and the effect of the fiber

Table 6: Elastic properties of the epoxy resin and the carbon fiber

Material	$E_{f1}$ (GPa)	$E_{f2}$ (GPa)	$G_{f12}$ (GPa)	$\mu_{f23}$	$\mu_{f12}$	$E_m$ (GPa)	$\mu_m$
AS4	234.6	13.8	13.8	0.25	0.2	—	—
Epoxy	—	—	—	—	—	2.94	0.35

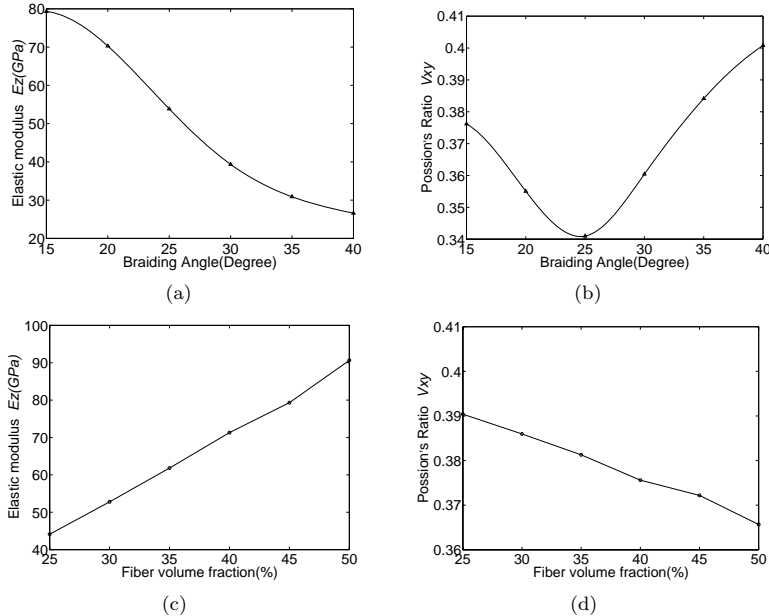


Figure 9: Variation of elastic constants with braiding angle and fiber volume fraction

volume fraction on the Poisson's ratio is relatively weak. Therefore, the results shown in Fig. 9 demonstrate that the braiding angle and fiber volume fraction are important factors affecting the mechanical properties and may be helpful to optimize the 3D 4-directional braided composite structures.

## 5 Conclusions

In this paper, a new parameterized microstructural unit cell model is established and the SOTS method is applied to predict the mechanical properties of 3D 4-directional braided composite materials, including the stiffness and strength parameters. UG is exploited secondly by Microsoft Visual Studio and the param-

eterized modeling of the unit cell is realized. And this model truly simulates the microstructure of the braided composites. Based on these unit cell models, the stiffness and strength parameters of 3D 4-directional braided composites are predicted by the SOTS method. The good agreement between the calculated results and experimental data demonstrates that the established unit cell model is applicable and the SOTS method is valid to predict the mechanical properties of 3D 4-directional braided composites. Moreover, the relations between different braiding angles and fiber volume fractions and the elastic constants are investigated. The results show that they are important factors affecting the mechanical properties and may be helpful to optimize the 3D 4-directional braided composite material structures.

**Acknowledgement:** This work is supported by the National Basic Research Program of China (973 Program 2012CB025904), the National Natural Science Foundation of China (90916027), and also supported by the State Key Laboratory of Science and Engineering Computing and Center for high performance computing of Northwestern Polytechnical University.

## References

- Chen, L.; Tao, X. M.; Choy, C. L.** (1999): Mechanical analysis of 3-d braided composites by the finite multiphase element method. *Composites Science and Technology*, vol. 59, no. 16, pp. 2383–2391.
- Cioranescu, D.; Donato, P.** (1999): *An introduction to homogenization*. Oxford University Press Oxford.
- Cui, J. Z.; Shin, T. M.; Wang, Y. L.** (1999): Two-scale analysis method for bodies with small periodic configuration. *Structural Engineering and Mechanics*, vol. 7, no. 6, pp. 601–614.
- Cui, J. Z.; Yu, X. G.** (2006): A two-scale method for identifying mechanical parameters of composite materials with periodic configuration. *Acta Mechanica Sinica*, vol. 22, no. 6, pp. 581–594.
- Fang, G. D.; Liang, J.** (2011): A review of numerical modeling of three-dimensional braided textile composites. *Journal of Composite Materials*, vol. 45, no. 23, pp. 2415–2436.
- Guedes, J. M.; Kikuchi, N.** (1990): Preprocessing and postprocessing for materials based on the homogenization method with adaptive finite element methods. *Computer methods in applied mechanics and engineering*, vol. 83, no. 2, pp. 143–198.

- Hou, T. Y.; Wu, X. H.** (1997): A multiscale finite element method for elliptic problems in composite materials and porous media. *Journal of computational physics*, vol. 134, no. 1, pp. 169–189.
- Kalidindi, S. R.; Abusafieh, A.** (1996): Longitudinal and transverse moduli and strengths of low angle 3-d braided composites. *Journal of composite materials*, vol. 30, no. 8, pp. 885–905.
- Kalidindi, S. R.; Franco, E.** (1997): Numerical evaluation of isostrain and weighted-average models for elastic moduli of three-dimensional composites. *Composites Science and Technology*, vol. 57, no. 3, pp. 293–305.
- Kang, T. J.; Kim, S.; Jung, K.** (2008): Analysis of geometrical parameters using a cad system for a 3-d braided preform. *Textile Research Journal*, vol. 78, no. 10, pp. 922–935.
- Ko, F. K.; Pastore, C. M.** (1985): Structure and properties of an integrated 3-d fabric for structural composites. *Recent advances in composites in the United States and Japan, ASTM STP*, vol. 864, pp. 428–439.
- Lu, Z. X.; Feng, Z. H.; Kou, C. H.; Liu, Z. G.; Lu, M.; Mai, H. C.; Tang, G. Y.** (1999): Studies on tensile properties of braided structural composite materials. *Acta Materiae Compositae Sinica*, vol. 16, no. 3, pp. 129–134.
- Ma, C. L.; Yang, J. M.; Chou, T. W.** (1986): Elastic stiffness of three-dimensional braided textile structural composites. *ASTM special technical publication*, , no. 893, pp. 404–421.
- Nagai, K.; Yokoyama, A.; Maekawa, Z.-i.; Hamada, H.; Noguchi, Y.** (1992): The study of analytical method for three-dimensional composite materials. *Transactions of the Japan Society of Mechanical Engineers*, vol. 58, no. 555, pp. 2099–2103.
- Pankow, M.; Waas, A. M.; Yen, C. F.** (2012): Modeling the response of 3d textile composites under compressive loads to predict compressive strength. *Computers, Materials, & Continua*, vol. 32, no. 2, pp. 81–106.
- Sun, H. Y.; Di, S. L.; Zhang, N.; Pan, N.; Wu, C. C.** (2003): Micromechanics of braided composites via multivariable fem. *Computers & structures*, vol. 81, no. 20, pp. 2021–2027.
- Wan, Q.; Li, F. G.; Liang, H.; Zhang, L. L.** (2005): Finite element simulation of key properties of three-dimensional and four-step braided composite. *Journal of Aeronautical Materials*, vol. 25, pp. 30–35.
- Wang, B.; Jiao, G. Q.; Tao, L.; Geng, X. L.** (2003): Bending experiment investigation of pr china's 3-d braided t300/qy9512 composite. *Journal Northwestern Polytechnical University*, vol. 21, no. 5, pp. 555–558.

- Wang, X. M.; Xing, Y. F.** (2010): Developments in research on 3d braided composites. *Acta Aeronautica et Astronautica Sinica*, vol. 31, pp. 914–927.
- Wang, Y. Q.; Sun, X. K.** (2001): Digital-element simulation of textile processes. *Composites science and technology*, vol. 61, no. 2, pp. 311–319.
- Wang, Y. Q.; Wang, A.** (1995): Microstructure/property relationships in three-dimensionally braided fiber composites. *Composites Science and Technology*, vol. 53, no. 2, pp. 213–222.
- Wang, Y. Q.; Zhang, L. T.; Cheng, L. F.** (2008): Computer geometry simulation of spatial structure of three-dimensional braided composites. *Journal of Aeronautical Materials*, vol. 28, pp. 95–98.
- Wu, D. I.; Hao, Z. P.** (1993): 5d braided structural composites. *Journal of Astronautics*, vol. 3, pp. 13–16.
- Yan, S.; Wu, Z. L.; Sun, Y. G.** (2007): Experimental investigation compressive mechanical properties of 3d 4-directional braided composite. *Journal of materials engineering*, vol. 7, pp. 59–63.
- Yang, C. K.** (2002): Research of mechanical properties of 3d braided composite materials. *Journal of materials engineering*, vol. 7, pp. 33–39.
- Yang, J. M.; Ma, C. L.; Chou, T. W.** (1986): Fiber inclination model of three-dimensional textile structural composites. *Journal of Composite Materials*, vol. 20, no. 5, pp. 472–484.
- Yang, Z. Q.; Cui, J. Z.; Nie, Y. F.; Ma, Q.** (2012): The second-order two-scale method for heat transfer performances of periodic porous materials with interior surface radiation. *CMES: Computer Modeling in Engineering & Sciences*, vol. 88, no. 5, pp. 419–442.
- Yu, X. G.; Cui, J. Z.** (2007): The prediction on mechanical properties of 4-step braided composites via two-scale method. *Composites science and technology*, vol. 67, no. 3, pp. 471–480.
- Zhang, C.; Xu, X. W.** (2012): Finite element analysis of 3d braided composites based on three unit-cells models. *Composite Structures*, vol. 98, pp. 130–142.